JOURNAL OF MATERIALS SCIENCE: MATERIALS IN MEDICINE 6 (1995) 258–265

Bond degradation at the plasma-sprayed HA coating/Ti–6Al–4V alloy interface: an *in vitro* study

C. Y. YANG
Department of Orthopedics, National Cheng Kung University Medical Center, Tainan, Taiwan

B. C. WANG, E. CHANG
Department of Materials Science and Engineering, National Cheng Kung University, Tainan, Taiwan

B. C. WU
Industrial Technology Research Institute, Hsinchu, Taiwan

The successful use of the plasma-sprayed HA-coated Ti–6Al–4V system requires strong adhesion between the ceramic coating and the underlying metal substrate. The aim of this study was to evaluate the bond strength at the HA coating (HAC)/Ti–6Al–4V interface, for specimens that had and had not been subjected to immersion in a pH-buffered, serum-added simulated body fluid (SBF). Moreover, coating characteristics affecting the mechanical stability after having been immersed in SBF were clarified. The results showed that bonding degradation of approximately 25–33% of the original strength was measured after immersion in SBF, and that this predominantly depended on the characteristics of the HAC and the period of immersion. Since the surface morphologies of HACs have dissolved in the SBF, it is suggested that the interlamellar structure of the HAC was weakened and, therefore, the bond strength degraded. As both the crystallinity and impurity phases of the HAC increased with immersion time, it can be concluded that the dissolution of the HAC resulting from the initial microstructure has overtaken that of the coating crystallinity and phase purity. A denser microstructure is required to ensure a satisfactory HAC/Ti–6Al–4V interface.

1. Introduction

Plasma-sprayed hydroxyapatite (HA)-coated Ti alloy implants, exhibiting excellent biocompatibility and satisfactory mechanical properties, are currently being investigated as an approach to achieving reliable implant-to-bone fixation, both in animal [1–10] and human clinical studies [11, 12]. In the majority of previous studies, the biological and biomechanical behaviours at the HA coating (HAC)/bone interface have favoured an encouraging result. However, in evaluating the performance and stability of HAC in the load-bearing situation after long-term follow-up, special consideration should be given to the HAC/Ti alloy interface.

Although there is evidence of a chemical reaction observed at the HAC/Ti alloy interface [13, 14], research suggests the presence of a potentially weak HAC/Ti alloy interface [13, 15–18], which may compromise the function of this device, particularly while the HACs are used as the primary means of fixation (i.e. no micro- or macro-textured bond coat enhancing the interfacial strength between HAC and Ti alloy substrate). In a study by Spivak *et al.* [17], the failure mode of bone-HAC interfacial tensile testing was observed to occur consistently at the HAC–Ti interface, indicating clearly that it was difficult to develop reliable HAC/Ti alloy bonding. Recently, using a modified short-bar technique for interfacial fracture toughness determination, Filiaggi *et al.* [13] showed that there existed relatively low fracture toughness values in an HA-coated Ti–6Al–4V implant system. Therefore, emphasis must be given to the promotion of bonding at the HAC/Ti alloy interface.

To improve HAC/Ti alloy bonding, some general guidelines have been proposed: (1) a denser microstructure (less porosity) would result in higher bonding strength [19]; (2) by overcoming the problems of stress concentration and low cohesive strength among interlamellar structure, thinner HAC (50–75 μm) displayed higher bonding strength [19, 20]; (3) bonding could be improved after heat treatment *in vacuo* by the formation of a titanium–phosphate phase at the interface [21]. Nevertheless, for clinical applications, the question arises whether the HAC/Ti alloy interface

0957–4530

would degrade with time in a physiological medium. Since signs of resorption of HACs have been documented [7, 9, 12, 22–23], the influence of the dissolution of HACs on the mechanical stability remains to be determined. Furthermore, changes in the coating characteristics after immersion in a physiologic medium have not yet been fully evaluated.

In this study, HACs that were quite different in microstructure, concentration of impurity phase, and index of crystallinity were used to evaluate bonding at the HAC/Ti alloy interface. Testing was done with and without simulated body fluid (SBF) immersion. The SBF employed was a pH value buffered, serum added physiological medium, different from the traditional salt medium. After 1, 2, 3, and 4 weeks of immersion, the bond strength at the HAC/Ti alloy interface was calculated by means of the adhesive test (ASTM C-633). Moreover, the changes in coating characteristics that influenced the stability in SBF were studied. This work expands upon the results of a previous study [24].

2. Materials and methods

2.1. Preparation of plasma-sprayed HACs

The feedstock HA powders and spraying conditions used have been reported elsewhere [24]. Three HACs with different coating characteristics were prepared (Table I) according to our previous work [24]: (1) H1-HAC with the most dense and molten microstructure, the highest concentration of impurity phases (CIP), and middle index of crystallinity (IOC); (2) H2-HAC with dense and molten microstructure, middle CIP, and the least ICO; (3) H3-HAC with the least dense and partially molten microstructure, the lowest CIP, and the best IOC. The surface morphologies of HACs with different degrees of melting are shown in Fig. 1. The CIP of HACs was defined as follows [24]:

$$\text{CIP} = (I_{\text{im}}/\text{I}_{\text{o}}) \times 100\%$$

where I_{im} was the sum of the main peak intensity of all impurity phases in each HAC and I_{o} was the main peak intensity of HA phase in the HA powders. The IOC of HACs was defined as follows [24]:

$$\text{IOC} = (I_{\text{c}}/I_{\text{o}}) \times 100\%$$

where I_{c} was the main peak intensity of the HA phase in each HAC. More detailed descriptions of the terms CIP and IOC are contained in a previous work [24].

TABLE I Characteristics of plasma-sprayed HACs used in this study

Parameter	HACs		
	H1	H2	H3
Porosity (%)	4	7	12
CIP (%)	14.5	13.3	4.5
IOC (%)	27.5	21.9	63.5

Note: CIP = Concentration of impurity phases
IOC = Index of crystallinity

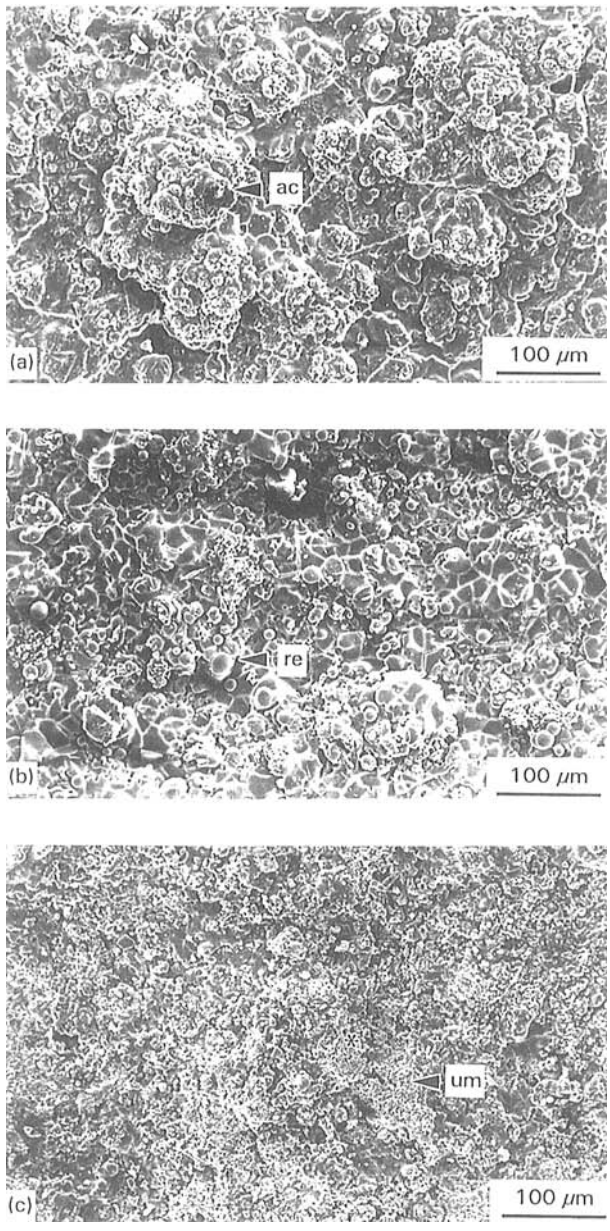

Figure 1 Surface morphologies of: (a) H1-HAC with molten and accumulated splats; (b) H2-HAC with molten and respherodized splats; (c) H3-HAC with unmelted powders. ac, accumulated splat; re, respheroidized splat; um, unmelted powders.

As illustrated by X-ray diffraction patterns in Fig. 2, the phase purity and the crystallinity of HACs used in this study differed from one another.

Two shapes of bioinert Ti–6Al–4V (ASTM F-136) were used as substrates: cylindrical rods, measuring 2.54 cm in diameter and 7.62 cm in length were used for bonding strength measurements. Plate specimens ($1 \times 1 \times 0.3$ cm) were employed for coating characterization.

2.2. Adhesion testing at the HAC/Ti–6Al–14V interface

2.2.1. Bond strength measurements in situ

The bond strength at the HAC/Ti–6Al–4V interface was tested using the adhesion test (ASTM C-633) which was especially designed for plasma-sprayed coatings. Each test specimen was an assembly comprising a substrate rod to which the HAC was applied,

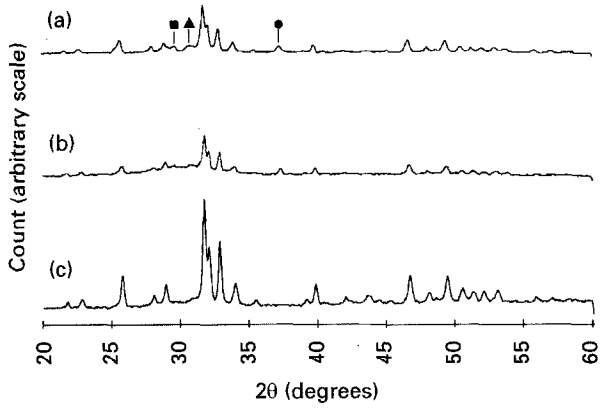

Figure 2 X-ray diffraction patterns of: (A) H1-HAC with many impurity phases; (b) H2-HAC with the least crystallinity; and (c) H3-HAC with few impurity phases and the best crystallinity. ▲ α, β-$Ca_3(PO_4)_2$ (TCP); ■ $Ca_4P_2O_9$ (TP); ● CaO.

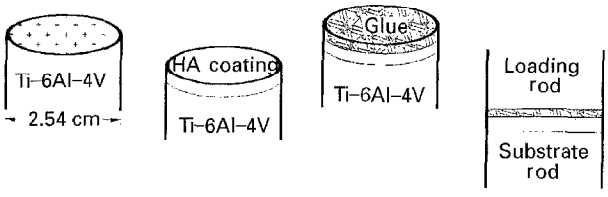

Figure 3 Schematic representation of the adhesive test (ASTM C-633): (a) degreased, gmt-blasted substrate rod; (b) plasma-sprayed HAC on substrate rod; (c) glue attached to HAC; (d) Loading rod attached on substrate rod.

and a loading rod (Fig. 3). H1–H3 coatings with the same thickness (approximately 200 μm) were plasma-sprayed on to the substrate rods (Fig. 3b), which had been degreased to remove organic contaminants and blasted with Al_2O_3 grit to provide surface roughness (Fig. 3a). The facings of the loading rods were then grit-blasted and attached to the surfaces of HACs using a special adhesive bonding glue (METCO EP-15, Fig. 3d). This segment was held perpendicularly and put into an oven at 180°C for 2 h. When the glue was cured and hardened, the segment was loaded in the Instron (Model 1125) machine to measure the tensile bond strength.

2.2.2. Bond strength measurements after immersion in SBF

The HA-coated substrate rods were cleaned using an ultrasonic wash in reagent grade acetone followed by an ultrasonic rinse in distilled water and then put into culture vials (100 ml). Prior to soaking, dry heat (120 °C, 8 h) sterilization was performed on the culture vials involving specimens. Under a sterile environment, the simulated body fluid (SBF) was added to the vials with 30 ml SBF/cm^2 of HAC. Complete SBF, that is, Dulbecco's Modified Eagle Media (DMEM, Gibco Lab., NY) supplemented with 10% fetal bovine serum (FBS, HyClone Lab. Inc., Utah), 2.2 g/l $NaHCO_3$, 0.1 g/l streptomycin sulfate, and 0.06 g/l penicillin was used for the experiments. The SBF was buffered at a pH of 7.2 with 5 N HCl. The vials were then placed in a humidified, 5% CO_2/balance air incubator to minimize the change in the initial pH; all immersions took place at 37°C without stirring.

After 1, 2, 3, and 4 weeks of immersion, the substrate rods were removed, washed with distilled water and dried in the oven. Then the substrate rods were attached to the facings of loading rods using adhesive agent to enable the bond strength measurements as described above. At each period, five specimens were tested. After the adhesive test, the failure mode at the Ti/HAC/agent region was evaluated.

2.3. Changes in characteristics of HACs after immersion in SBF

HA-coated plate specimens were employed to investigate the changes in characteristics after being immersed in SBF. The soaked sequences used were similar to those for rod specimens as described above. After periods of 1, 2, 3, and 4 weeks, the specimens were removed from the SBF and examined for coating characterization, including microstructure, phase purity and crystallinity. The surface morphologies of HACs were examined by scanning electron microscope (SEM, JEOL, JSMr 840). The phases of HACs were identified by X-ray diffractometer (XRD, Rigaku D/MAX III. V) with a scan speed of 4°/min between 20° and 60° (2θ angle), using CuK_α radiation. To judge the change in phase purity and crystallinity, CIP and IOC values of HACs at each immersion period were compared.

3. Results

3.1. Bonding strength measurements

The bond strength data measured from the adhesion tests are listed in Table II. At time zero (initial testing), it was found that the trend for bonding strength was: H1-HAC > H2-HAC > H3-HAC. A maximum bond strength of 30.98 ± 1.12 MPa (mean ± SD) for H1-HAC was reached.

Following immersion in SBF, the bond strengths of the HACs were found to degrade to different extents. For H1-HAC, a continuous degradation was noted from 29.36 ± 3.67 MPa at 1 week to 21.39 ± 1.34 MPa at 4 weeks. During the first week, degradation could be ignored. However, a total of about 30% reduction in bond strength was measured after 4 weeks of immersion. For H2-HAC, the degradation behaviour showed little difference from that of H1-HAC. Bond strength reduced from the start and the continuous degradation proceeded into the third week. At 4 weeks, the strength data increased as compared to that at 3 weeks. A value of approximately 25% reduction in strength was calculated 3 weeks post-immersion. With respect to H3-HAC, it is worth noting that the strength decreased significantly after 1 week immersion (about 33% reduction of original strength), revealing great differences from the other HACs. Moreover, compared to the data at week 1, an abnormal increase in strength data was observed after 2 weeks of immersion, and this level of strength was maintained up to the fourth week of immersion.

After the adhesion test, a typical failure mode at the HAC/Ti-6Al-4V interface is shown in Fig. 4a. A mix

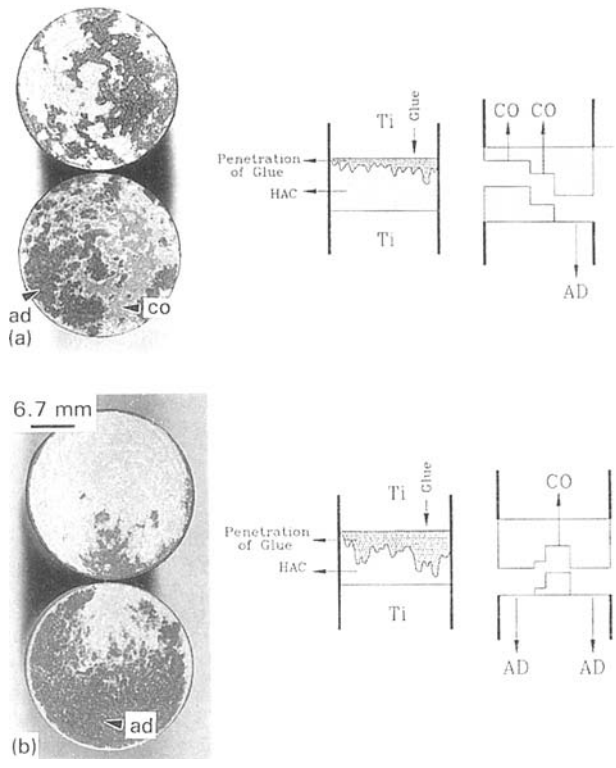

Figure 4 Fractographs and schematic representations of HACs after the adhesive test. A mixed failure mode revealing adhesive and cohesive failure was commonly observed (a). However, for HACs showing abnormal increase in strength data, more adhesive failure was observed (b). co, cohesive failure; ad, adhesive failure.

of adhesive (coating–substrate) and cohesive (lamellar coatings themselves) failure was observed at the interface. These findings indicated that the results of this adhesive test were meaningful and matched well with the criteria of ASTM C-633. However, for specimens showing abnormal increase in strength data after being immersed in SBF, more adhesive failures were found (Fig. 4b).

3.2. Coating characterization after immersion in SBF

3.2.1. Surface morphologies of HACs

Following immersion in SBF, the surface morphologies of HACs dissolved to different degrees. Predominantly, this depended on the kind of HAC and the length of time of immersion. It is shown in Fig. 5 that the morphologies of H1-HACs revealed little change up to 4 weeks of immersion (compare with Fig. 1a).

Throughout the immersion periods, only slight surface etching was observed. However, for H2-HAC as shown in Fig. 6, the degree of surface attack by the SBF was clearly evident. At week 1, in comparison with Fig. 1b, the coating displayed more microcracks on the surface (Fig. 6a). After 3 weeks of immersion, many circulated splats of around 10 μm were isolated from the cracked matrix (Fig. 6b). With increasing immersion time, up to the fourth week, a smashed surface was found (Fig. 6c); the microstructure constructed was so weak that it could not withstand the bombardment of the electron beam under the scanning electron microscope. Since the microstructure of

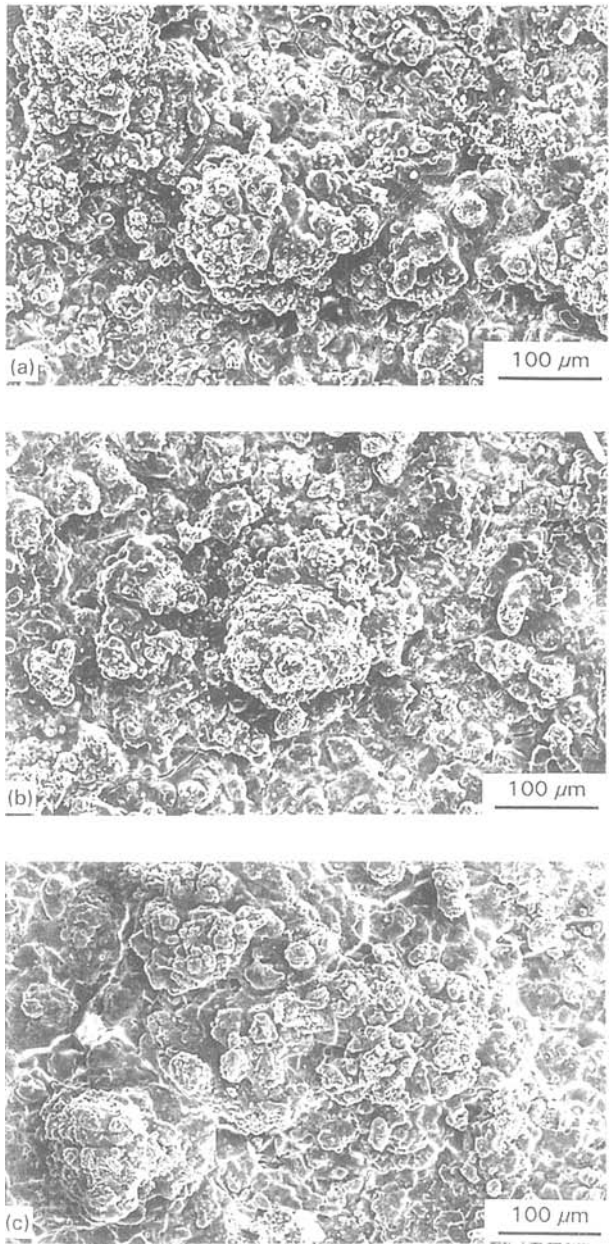

Figure 5 The surface morphologies of H1-HACs after (a) 1 week; (b) 3 weeks; and (c) 4 weeks of immersion. Only slight etched morphologies were observed.

H3-HAC was loosely constructed (Fig. 1c), it is apparent from Fig. 7a that the H3-HAC has been seriously attacked by the SBF after only 1 week of immersion. The unmelted HA particles observed before immersion in the SBF (Fig. 7c) have, for the most part, dissolved after 1 week (Fig. 7b). When the immersion time exceeded 2 weeks, the microstructure of H3-HAC could not withstand the damage caused by the electron beam, and no further observations of surface morphology were possible.

3.2.2. Phase concentration and crystallinity of HACs

The XRD patterns of HACs after having been immersed in SBF are shown in Figs 8–10. The IOC and CIP values calculated from these XRD patterns are shown in Fig. 11 and Fig. 12, respectively. It is apparent from Fig. 11 that, for each kind of HAC, the crystallinity

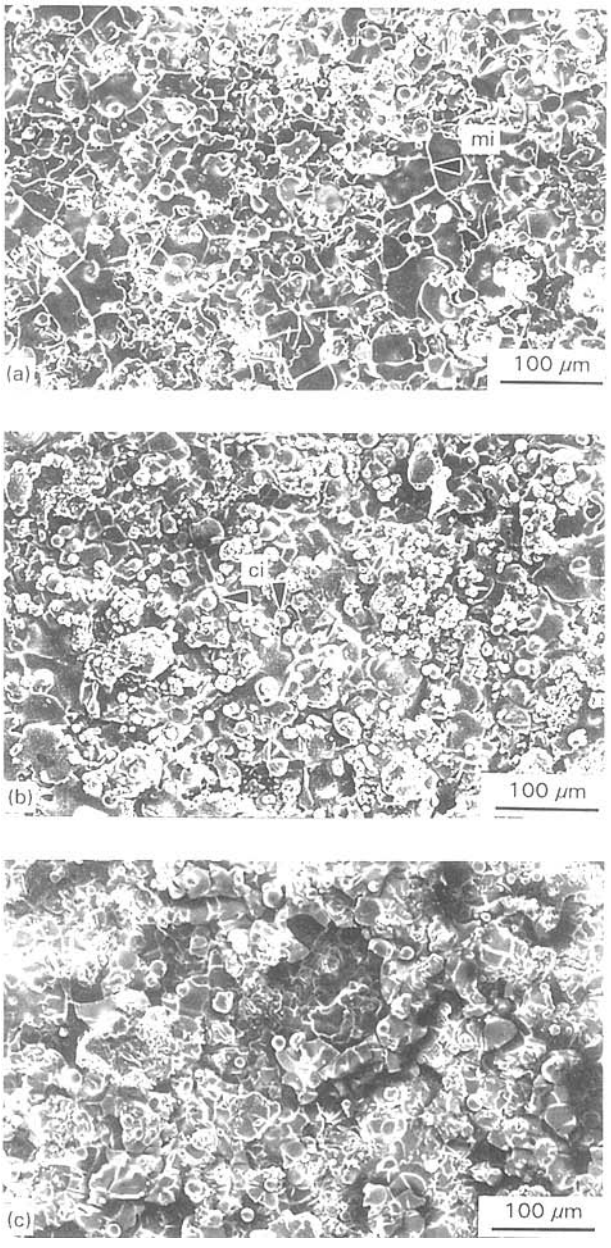

Figure 6 The surface morphologies of H2-HACs after (a) 1 week; (b) 3 weeks; and (c) 4 weeks of immersion. Microcracks or circulated splats were found. mi, microcrack; ci, circulated splat.

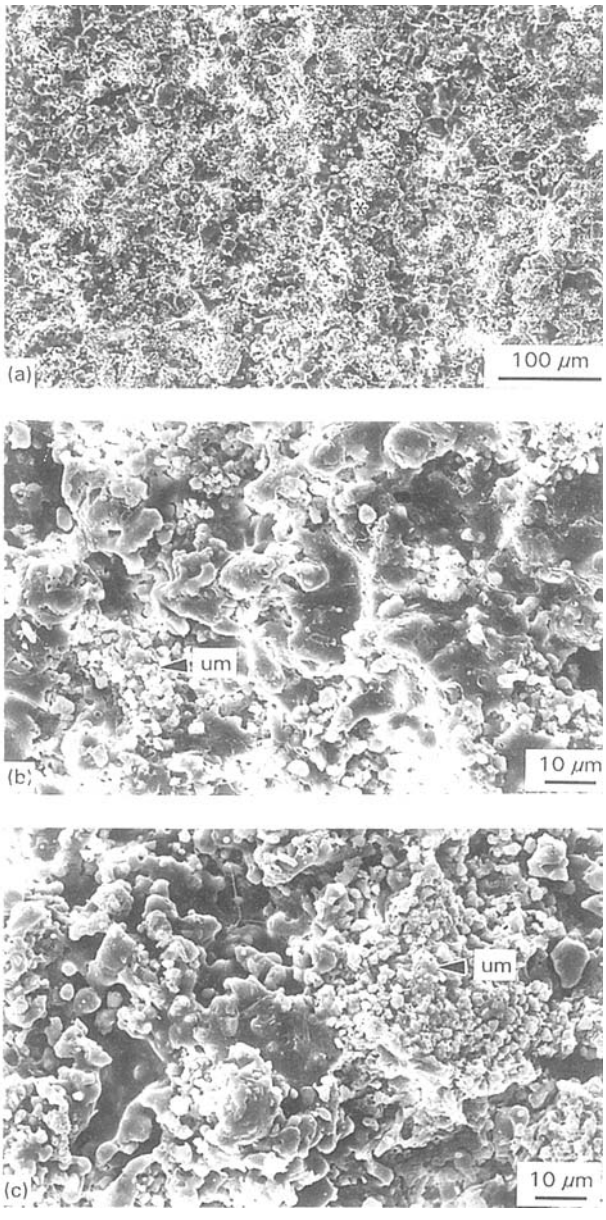

Figure 7 The change of surface morphologies of H3-HACs after immersion: (a) at 1 week showing many unmelted HA powders had dissolved after being soaked in SBF; (b) high magnification of star mark in (a); and (c) high magnification of star mark in Fig. 1c before immersion in the SBF. um, unmelted powders.

increased significantly following immersion in SBF. This finding was consistent with de Groot *et al.* [25], who reported that coating crystallinity increased after incubation in Gomoris buffer (pH = 7.2) for 4 weeks. For H3-HAC, a crystallinity index as high as 90% of original crystallinity of HA powders was reached after only 1 week of immersion.

On the other hand, as shown in Fig. 12, the impurity phases for H1- and H2-HACs also increased after immersion in the SBF. Nevertheless, a decrease in the concentration of impurity phases for H3-HACs was noted. It is theoretically recognized that plasma-sprayed HACs consist of crystalline and amorphous components. Each component might contain several phases. As the amorphous HA has crystallized after incubation in the SBF, the impurity phase in the amorphous component would also crystallize. This accounted for the increase in impurity phase for H1- and H2-HAC following immersion in the SBF.

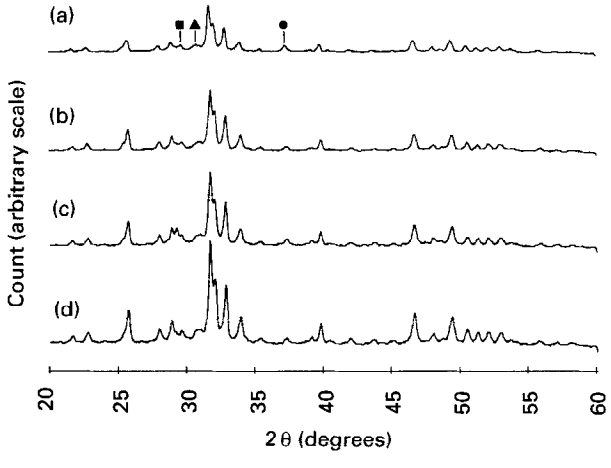

Figure 8 The XRD patterns of H1-HACs; (a) initial time; (b) 1 week; (c) 3 weeks; and (d) 4 weeks post-immersion. Both the index of crystallinity and the concentration of impurity phases increased noticeably after incubation in SBF. ▲ α, β-$Ca_3(PO_4)_2$ (TCP); ■ $Ca_4P_2O_9$ (TP); ● CaO.

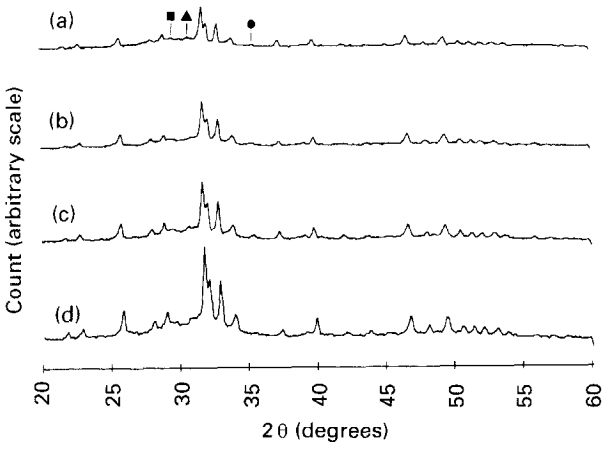

Figure 9 The XRD patterns of H2-HACs; (a) initial time; (b) 1 week; (c) 3 weeks; and (d) 4 weeks post-immersion. Both the index of crystallinity and the concentration of impurity phases increased after incubation in SBF. ▲ α, β-$Ca_3(PO_4)_2$ (TCP); ■ $Ca_4P_2O_9$ (TP); ● CaO.

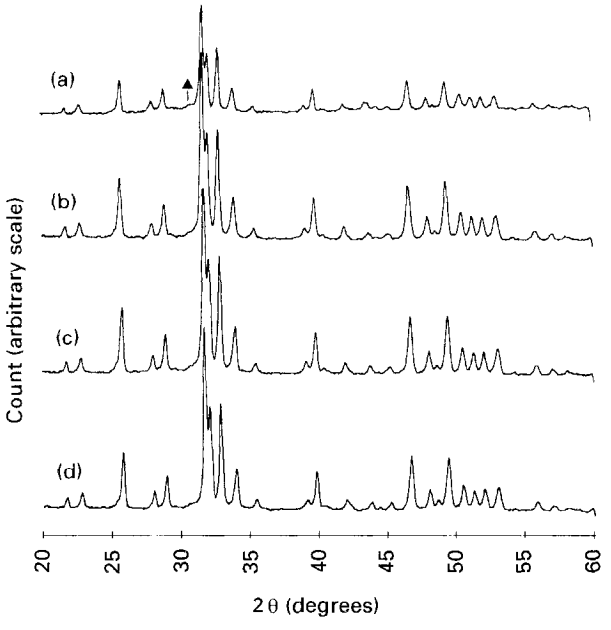

Figure 10 The XRD patterns of H3-HACs: (a) initial time; (b) 1 week; (c) 3 weeks; and (d) 4 weeks post-immersion. The coating crystallinity increased, but the concentration of impurity phases decreased. ▲ α, β-$Ca_3(PO_4)_2$ (TCP); ■ $Ca_4P_2O_9$ (TP); ● CaO.

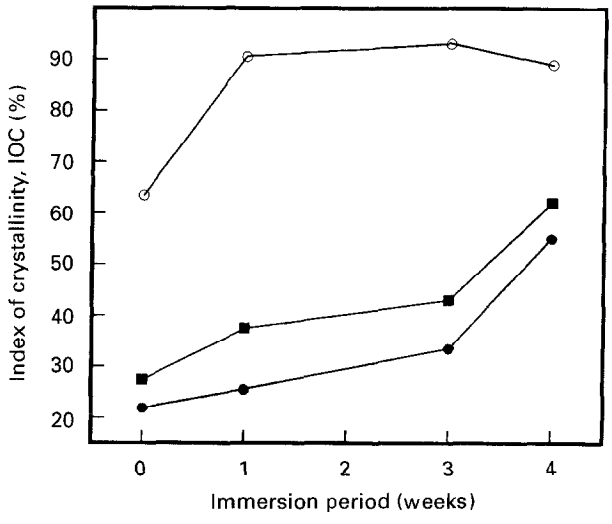

Figure 11 Relationship between IOC values and period of immersion (■ H1-HAC; ● H2-HAC; ○ H3-HAC). The coating crystallinity increased considerably after immersion in SBF.

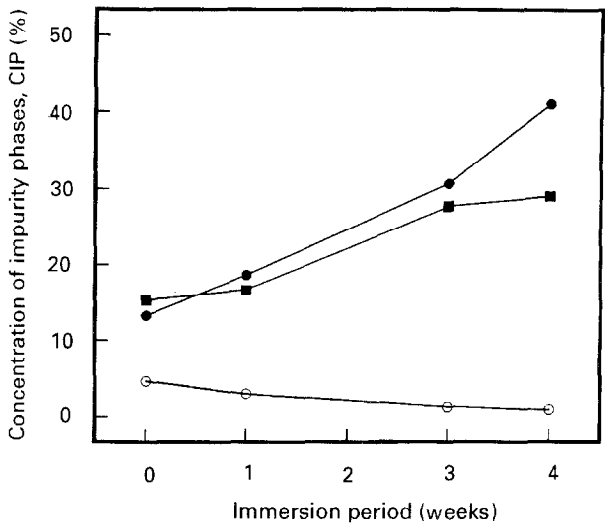

Figure 12 Relationship between CIP values and period of immersion (■ H1-HAC; ● H2-HAC; ○ H3-HAC). The concentration of impurity phases increased primarily after incubation in SBF.

However, with respect to H3-HAC, the decrease in impurity phases might be attributed to the fact that it revealed high purity in phases (Table I) before being immersed in SBF.

4. Discussion

Bond strength at the HAC/Ti–6Al–4V interface was evaluated, with and without SBF immersion. Some variables, including coating characteristics, that influenced the results of strength data before and after incubation in the SBF are discussed. This work represents a continuation of a previous characterization study of plasma-sprayed HA-coated Ti–6Al–4V systems.

It is generally believed that the true bond strength of plasma-sprayed coatings is a manifestation of mixed cohesive (lamellar layers themselves) and adhesive (coating to substrate) strength [19]. Therefore, as the adhesive test (ASTM C-633) was employed, the results of bond strength were suggested to be governed by a number of factors: (1) the thickness of the ceramic coating; (2) the properties (viscosity, adhesive strength, and shrinkage rate) of the glue employed; (3) the surface conditions (roughness and cleaning) of the metal substrate; (4) the interlamellar cohesive strength of the coating; and (5) the penetration of the glue into the imperfections (porosities and microcracks) of the coating. A thinner coating (less than 100 μm) would result in a higher bond strength partly because the measured strength data represented the strength of penetrated glue rather than the true bond strength of the coating [19, 20, 25]. This thickness effect could be judged from the fractography of tested rods which showed that the failure site occurred consistently at the glue/HAC interface [19]. In a study by Filiaggi and coworkers [13], the effect of the properties of adhesive glue on the bond strength was evident. They used high viscosity, quick-setting, but weaker strength glue and obtained lower bond strength (6.7 ± 1.5 MPa). However, this level of strength data might represent mostly the interlamellar cohesive

strength due to the fact that the glue was a quick-setting type. In the same study by Filiaggi *et al.* [13], a decrease both in fracture toughness values and bond strength data was reported when a lower surface roughness Ti–6Al–4V substrate was used. As a consequence, a suitable surface roughness combined with clean surface (no grits embedded) is required for preparing the Ti–6Al–4V substrate.

In this study, to prevent the influence of the thickness effect, HACs with a thickness of approximately 200 μm were employed. The adhesive glue (METCO EP-15) with low viscosity, slow-setting time, and high adhesive strength (50–60 MPa) was chosen, being similar to that used in other studies [20, 25]. Moreover, a well cleaned and fine-grit-blasted Ti–6Al–4V (surface roughness $R_a = 3.78 \pm 0.34\mu m$) substrate was prepared [10]. Therefore, it is deduced that the interlamellar cohesive strength might play a key factor in evaluating the bond strength in our HA-coated Ti–6Al–4V system. Since the H1-HAC had the most dense micro-structure (Fig. 1a) before immersion in SBF, it is not surprising that the highest bond strength (30.98 ± 1.12 MPa) was measured owing to H1-HAC having the highest interlamellar cohesive strength.

Following immersion in SBF, factors affecting the bond strength of HACs need rethinking. Since the surface morphologies of HACs were etched or dissolved by the SBF (Figs. 5–7), it is reasonable to suggest that the interlamellar cohesive strength was weakened. Consequently, the penetration of the glue into the imperfections should be of concern. If the coatings were just etched (H1-HAC during all immersed periods) or only slightly dissolved (H2-HAC during the first 3 weeks, H3-HAC at 1 week), the bond strength would decrease with immersed period owing to the weakened interlamellar cohesive strength. However, for coatings revealing significantly dissolved morphologies (H2-HAC at 4 weeks, H3-HAC during the last 3 weeks), excessive glue penetrating into the coating could affect the results considerably; abnormally increasing bond strengths with immersion time could come, for example, from: (1) the filling of porosities and microcracks; (2) the reinforcement of weakened interlamellar structure; or (3) bonding between the penetrated glue and the underlying Ti–6Al–4V substrate. Specifically, more adhesive failures would be observed from the fractography (Fig. 4b).

Since bonding degradation originated evidently from the dissolution of HACs, it is supposed that coating characteristics, including microstructure, crystallinity and phase concentration, could influence the dissolution rate of HACs in SBF and, thereafter, affect the bond strength. It has been generally recognized that the denser (less porosity) the HA bulk ceramic, the higher the stability would be in a physiological medium [26]. In the same way, HACs with denser microstructure would lead to less instability. This rationale could explain why the most dense H1-HAC dissolved only slightly (Fig. 5) and, consequently, only a 30% reduction of original bond strength was measured after 4 weeks of immersion (Table II). In contrast, for H3-HAC constructed with the least dense microstructure, a higher bonding degradation (33% reduction at 1 week) which resulted from serious dissolution (Fig. 7a) was evident, although an abnormal increase in strength data, contributed by the penetrated glue, was measured during the last 3 weeks in SBF.

The coating crystallinity, as quantitatively represented in the IOC value in this study, might prove to be of importance owing to the decreased dissolution rate when compared with poorly crystallized HACs [6]. This meant that the H2-HAC with the lowest IOC value (Table I) was suggested to be more bioresorbable. Although the H2-HAC was dissolved by the SBF (Fig. 6), it was not the most serious case. On the contrary, H3-HAC with the highest IOC value (Table I) was found to be the least stable (Fig. 7a). This observation contributed to the fact that, in evaluating the dissolving behaviour of HACs, the constructed microstructure rather than coating crystallinity seemed to be the most important variable in this short-term *in vitro* study. In addition, as the amorphous component of HACs could crystallize in SBF (Fig. 11), initial crystallinity thus became less important. Therefore, it can be concluded that the coating crystallinity was not the most significant contributing factor to bonding degradation in SBF.

After spraying, impurity phases such as tricalcium phosphate (TCP), tetracalcium phosphate (TP) and calcium oxide have been documented to be hardly avoidable [27, 28]. Since the TCP and TP phase were reported to be quickly bioresorbed [26, 29–31], H1-HAC with high concentration of impurity phases (Table I) was suspected to reveal a high dissolution rate, especially when the impurity phases have significantly increased after being immersed in SBF (Fig. 12). However, according to the slight etched morphologies (Fig. 5) and the measured strength data (Table II), H1-HAC was the least degraded. The influence of purity on the dissolution rate was thus limited compared to the influence of the constructed microstructure.

As suggested by de Groot *et al.* [26], the physiochemical dissolution rate of HA bulk ceramic is also determined by the pH and chemical composition

TABLE II Results of bond strength measurements following immersion in SBF

HAC	Zero	Bond strength (MPa) after period of immersion			
		1 Week	2 Weeks	3 Weeks	4 Weeks
H1	30.98 ± 1.12	29.36 ± 3.67	26.30 ± 1.76	24.59 ± 2.54	21.39 ± 1.34
H2	28.31 ± 2.21	25.17 ± 0.76	23.23 ± 3.54	21.78 ± 1.07	23.85 ± 0.75
H3	27.34 ± 2.02	18.17 ± 0.96	25.73 ± 1.74	24.46 ± 2.65	25.17 ± 0.86

Values are given as mean ± SD after five tests.

of the incubating fluid (including composition of buffer). They showed that the dissolution rate of HA at pH 7.2 varied from 97.4 ppm of Ca ion, when buffered in citrate, to 44.3 ppm of Ca ion in Gomoris buffer [25]. In this study, pH-buffered and serum-added DMEM was used owing to the fact that it could simulate most accurately true body fluid. Nevertheless, bonding degradation in other simulated media should be further evaluated.

From the results of our previous study [24], plasma-sprayed HACs might display different coating characteristics, primarily depending on the spraying parameters used. In this study, we have clarified that, among coating characteristics, the constructed microstructure was the key factor in influencing bonding degradation in SBF. Therefore, the denser the microstructure, the lower the risk of bonding degradation. However, this kind of HAC has been demonstrated to contain a lower index of crystallinity and a higher concentration of impurity phases. Whether or not these undesired characteristics would influence the biological responses *in vivo* should be further investigated, since the ultimate strength of this HA-coated Ti–6Al–4V implant system to bone relied on both the HAC/Ti–6Al–4V and the HAC/bone interface.

5. Conclusion

A considerable effort has been made, using the *in vitro* method, to evaluate the bonding at the HAC/-Ti–6Al–4V interface, which may represent the weak link in implants of such surface design. The most important point elucidated in this study was the degradable bonding that existed at this interface, as suggested by the adhesive bond testing after being immersed in SBF. A range of 25–33% or higher reduction in bond strength was measured. Evidence of dissolved morphologies of HACs that weakened the interlamellar strength accounted for the degraded bond strength.

Additionally, it has been clarified that, among coating characteristics, the constructed microstructure was the major factor to affect dissolution of HACs and, consequently, bonding degradation of HACs. Finally, it should be made very clear, that, in any attempt to improve the performance of this HA-coated Ti–6Al–4V implant system, stability at the HAC/Ti–6Al–4V interface would be of paramount importance. As a result, a more dense HAC is needed.

Acknowledgements

The authors would like to thank Mr T. M. Lee and Mr M. L. Tsai for their technical assistance in sample preparation. This study was performed in cooperation with the Industrial Technology Research Institute, Hsinchu, Taiwan.

References

1. M. S. BLOCK, J. N. KENT and J. F. KAY, *J. Oral Maxillofac. Surg.* **45** (1987) 601.
2. R. G. T. GEESINK, K. de GROOT and C. P. A. T. KLEIN, *J. Bone Joint Surg.* **70B** (1988) 17.
3. S. D. COOK, K. A. THOMAS, J. F. KAY and M. JARCHO, *Clin. Orthop.* **232** (1988) 225.
4. D. P. RIVERO, J. FOX, A. K. SKIPOR, R. M. URBAN and J. O. GALANTE, *J. Biomed. Mater. Res.* **22** (1988) 191.
5. K. SOBALLE, E. S. HANSEN, H. B. RASMUSSEN, C. M. PEDERSEN and C. BUNGER, *Acta Orthop. Scand.* **61** (1990) 299.
6. D. BUSER, R. K. SCHENK, S. STEINEMANN, J. P. FIORELLINI, C. H. FOX and H. STICH, *J. Biomed. Mater. Res.* **25** (1991) 889.
7. J. A. JANSEN, J. P. C. M. van de WAERDEN, J. G. C. WOLKE and K. de GROOT, *ibid.* **25** (1991) 973.
8. M. GOTTLANDER and T. ALBREKTSSON, *Int. J. Oral Maxillofac. Imp.* **6** (1991) 339.
9. B. C. WANG, E. CHANG, D. TU and C. Y. YANG, *J. Mater. Sci. Mater. Med.* **4** (1993) 394.
10. B. C. WANG, E. CHANG and C. Y. YANG, *J. Biomed. Mater. Res.* **27** (1993) 1315.
11. R. G. T. GEESINK, *Clin. Orthop.* **261** (1990) 39.
12. T. W. BAUER, R. G. T. GEESINK, R. ZIMMERMAN and J. T. McMAHON, *J. Bone Joint Surg.* **73A** (1991) 1439.
13. M. J. FILIAGGI, N. A. COOMBS and R. M. PILLIAR, *J. Biomed. Mater. Res.* **25** (1991) 1211.
14. H. JI, C. B. PONTON and P. M. MARQUIS, *J. Mater. Sci. Mater. Med.* **3** (1992) 283.
15. M. L. FILIAGGI, N. A. COOMBS and R. M. PILLIAR, *Mater. Res. Soc. Symp. Proc.* **153** (1989) 377.
16. R. M. PILLIAR, D. A. DEPORTER, P. A. WATSON, M. PHAROAH, M. CHIPMAN, N. VALIQUETTE, S. CARTER and K. de GROOT, *J. Dent. Res.* **70** (1991) 1338.
17. J. M. SPIVAK, J. L. RICCI, N. C. BLUMENTHAL and H. ALEXANDER, *J. Biomed. Mater. Res.* **24** (1990) 1121.
18. S. D. COOK, J. F. KAY, K. A. THOMAS and M. JARCHO, *Int. J. Oral Maxillofac. Imp.* **2** (1987) 15.
19. B. C. WANG, E. CHANG, C. Y. YANG, D. TU and C. H. TASI, *Surf. Coat. Technol.* **58** (1993) 107.
20. E. MUNTING, M. VERHELPEN, F. LI and A. VINCENT, in "*CRC handbook of bioactive ceramics*", edited by T. Yamamuro, L. L. Hench and J. Wilson (CRC Press, Florida, 1990) pp. 143–148.
21. H. JI and P. M. MARQUIS, *Biomaterials* **14** (1993) 64.
22. W. J. A. DHERT, C. P. A. T. KLEIN, J. G. C. WOLKE, E. A. van der VELDE and K. de GROOT, *J. Biomed. Mater. Res.* **25** (1991) 1183.
23. C. P. A. T. KLEIN, P. PATKA, H. B. M. van der LUBBE, J. G. C. WOLKE and K. de GROOT, *ibid.* **25** (1991) 53.
24. C. Y. YANG, B. C. WANG, E. CHANG and J. D. WU, *J. Mater. Sci. Mater. Med.* **6** (1995) 249.
25. K. de GROOT, C. P. A. T. KLEIN, J. G. C. WOLKE and J. M. A. de BLIECK-HOGERVORST, in "*CRC handbook of bioactive ceramics*", edited by T. Yamamuro, L. L. Hench and J. Wilson (CRC Press, Florida, 1990) pp. 133–142.
26. *idem., ibid.* pp. 3–16.
27. P. DUCHEYNE, J. CUCKLER, S. RADIN and E. NAZAR, *ibid.* pp. 123–131.
28. K. A. GROSS and C. C. BERNDT, *Proceedings of 2nd Plasma-Technik Symposium* Plasma-Technik AG, Wohlen **3** (1991) 159.
29. K. SHIMAZAKI and V. MOONEY, *J. Orthop. Res.* **3** (1985) 301.
30. P. S. EGGLI, W. MULLER and R. K. SCHENK, *Clin. Orthop.* **232** (1988) 127.
31. L. XIE and E. A. MONROE, in "*CRC handbook of bioactive ceramics*", edited by T. Yamamuro, L. L. Hench and J. Wilson (CRC Press, Florida, (1990) pp. 29–37.

Received 18 October 1993
and accepted 14 June 1994